Received: 15 February 2021 | Revised: 9 July 2021 | Accepted: 20 July 2021

DOI: 10.1002/hbm.25612

RESEARCH ARTICLE

WILEY

Early motor network connectivity after stroke: An interplay of general reorganization and state-specific compensation

Theresa Paul[1] | Lukas Hensel[1] | Anne K. Rehme[1] | Caroline Tscherpel[1] | Simon B. Eickhoff[2,3] | Gereon R. Fink[1,4] | Christian Grefkes[1,4] | Lukas J. Volz[1,4]

[1]Department of Neurology, University Hospital Cologne, Cologne, Germany

[2]Institute of Neuroscience and Medicine, Brain & Behaviour (INM-7), Research Centre Juelich, Juelich, Germany

[3]Institute of Systems Neuroscience, Medical Faculty, Heinrich Heine University Duesseldorf, Duesseldorf, Germany

[4]Institute of Neuroscience and Medicine, Cognitive Neuroscience (INM-3), Research Centre Juelich, Juelich, Germany

Correspondence
Lukas J. Volz, Department of Neurology, University of Cologne, Kerpener Str. 62, 50937 Cologne, Germany.
Email: lukas.volz@uk-koeln.de

Funding information
Deutsche Forschungsgemeinschaft, Grant/Award Numbers: 431549029-SFB 1451, RE3014/2-1; Horizon 2020 Framework Programme, Grant/Award Numbers: 785907 (HBP SGA2), 945539 (HBP SGA3); Marga and Walter Boll Stiftung

Abstract

Motor recovery after stroke relies on functional reorganization of the motor network, which is commonly assessed via functional magnetic resonance imaging (fMRI)-based *resting-state functional connectivity (rsFC)* or *task-related effective connectivity (trEC)*. Measures of either connectivity mode have been shown to successfully explain motor impairment post-stroke, posing the question whether motor impairment is more closely reflected by rsFC or trEC. Moreover, highly similar changes in ipsilesional and interhemispheric motor network connectivity have been reported for both rsFC and trEC after stroke, suggesting that altered rsFC and trEC may capture similar aspects of information integration in the motor network reflecting principle, state-independent mechanisms of network reorganization rather than state-specific compensation strategies. To address this question, we conducted the first direct comparison of rsFC and trEC in a sample of early subacute stroke patients ($n = 26$, included on average 7.3 days post-stroke). We found that both rsFC and trEC explained motor impairment across patients, stressing the clinical potential of fMRI-based connectivity. Importantly, intrahemispheric connectivity between ipsilesional M1 and premotor areas depended on the activation state, whereas interhemispheric connectivity between homologs was state-independent. From a mechanistic perspective, our results may thus arise from two distinct aspects of motor network plasticity: task-specific compensation within the ipsilesional hemisphere and a more fundamental form of reorganization between hemispheres.

KEYWORDS
brain network connectivity, dynamic causal modeling (DCM), ischemic stroke, motor network reorganization, resting-state fMRI

1 | INTRODUCTION

Motor recovery after stroke relies on various intra- and inter-hemispheric processes aiming at compensating the loss of specialized neural tissue, commonly referred to as *functional reorganization* (Cramer, 2008). In humans, cerebral reorganization can be assessed by functional magnetic resonance imaging (fMRI) and specifically by the analysis of connectivity, that is, changes in inter-regional interactions (Grefkes & Fink, 2014). In particular, two fMRI-based connectivity approaches have frequently revealed changes in the motor network

after stroke: *resting-state functional connectivity (rsFC)* and *task-related effective connectivity (trEC)*. rsFC is typically estimated via temporal correlations between time series of different brain regions recorded at rest. It can be easily acquired even in severely affected patients, but is highly susceptible to confounds such as head motion (Power et al., 2014; Thiel & Vahdat, 2015). trEC describes the causal influence one brain region exerts on another (Friston, 1994). It is commonly estimated during task performance using Dynamic Causal Modeling (DCM), a model-based framework conceptualizing connectivity as directed facilitatory or inhibitory influences (Buxton, Wong, & Frank, 1998; Friston, Harrison, & Penny, 2003; Stephan & Friston, 2010). While trEC enables more specific insights regarding the nature of connectivity and causality, results are highly task- and model-dependent, which may limit their generalizability (Friston et al., 2003).

Assessing motor network connectivity during unilateral hand movements in healthy subjects, DCM has repetitively shown positive, excitatory coupling from bilateral premotor areas onto the primary motor cortex (M1) contralateral to the moving hand and negative, inhibitory coupling from the contralateral to the ipsilateral M1 (Grefkes, Eickhoff, Nowak, Dafotakis, & Fink, 2008; Pool, Rehme, Fink, Eickhoff, & Grefkes, 2013; Rehme, Eickhoff, Wang, Fink, & Grefkes, 2011; Volz, Sarfeld, et al., 2015). In the acute and subacute phase post-stroke, the excitatory influence from ipsilesional premotor areas onto ipsilesional M1 has been reported to be reduced, resulting in decreased excitation of the ipsilesional M1 during paretic hand movements (Rehme, Eickhoff, et al., 2011). Moreover, the inhibitory influences typically observed from ipsilesional M1 and premotor areas onto contralesional M1 were attenuated (Rehme, Eickhoff, et al., 2011). Importantly, altered trEC has been linked to stroke-induced motor impairment: ipsilesional influences of premotor areas on M1 and interhemispheric inputs onto contralesional M1 were related to motor performance and functional recovery (Grefkes et al., 2010; Grefkes & Ward, 2014; Rehme, Eickhoff, et al., 2011; Volz, Sarfeld, et al., 2015). Motor network alterations assessed via rsFC feature a characteristic time-course of changes deemed to reflect functional reorganization (Grefkes & Fink, 2014). Interhemispheric rsFC between bilateral motor areas, especially between bilateral M1, first decreases and subsequently re-increases alongside functional recovery, thereby resembling interhemispheric trEC changes (Carter et al., 2009, 2012; Golestani, Tymchuk, Demchuk, & Goodyear, 2013; Park et al., 2011; van Meer et al., 2010, 2012; Zheng et al., 2016). Moreover, increased rsFC between ipsilesional premotor areas and M1 has been found post-stroke and has also been linked to behavioral performance in line with findings obtained from DCM studies (Lee et al., 2017; Rehme, Volz, Feis, Bomilcar-Focke, et al., 2015; Volz et al., 2016).

In summary, both approaches highlight changes in ipsilesional premotor–M1 as well as interhemispheric motor network connectivity in the subacute phase post-stroke that relate to motor performance of the paretic hand. However, it remains unclear whether rsFC or trEC is better suited to explain motor impairment in (sub)acute stroke with implications for potential clinical applications. From a mechanistic perspective, the similarity of post-stroke changes in motor network connectivity between rsFC and trEC leads to the question whether some fundamental aspects of stroke-induced changes in information integration may be similarly captured during rest and task-performance, that is, in a state-independent fashion by both rsFC and trEC. Conversely, both approaches probe the brain during vastly different physiological states: while rsFC describes the brain during wakeful rest, trEC reflects network interactions underlying the performance of a given task, resulting in largely unrelated motor network rsFC and trEC in healthy subjects (Rehme, Eickhoff, & Grefkes, 2013).

To address these questions, we here for the first time directly compared rsFC and trEC in a group of 26 acute to early subacute stroke patients tested within the first two weeks post-stroke. First, we probed the potential of both connectivity approaches to explain variance in motor impairment. Considering that trEC-estimates are based on data recorded during the performance of an active motor task, we expected trEC to be more closely related to motor performance than rsFC. Next, we assessed which aspects of both connectivity approaches were best suited to explain motor performance. Considering previous findings after stroke, we hypothesized that interhemispheric M1–M1 connectivity would be particularly relevant for both rsFC and trEC (Carter et al., 2009, 2012; Golestani et al., 2013; Park et al., 2011; van Meer et al., 2010, 2012; Zheng et al., 2016), while the driving input from ipsilesional premotor areas onto the affected M1 should be of particular importance for trEC (Grefkes et al., 2010; Grefkes & Ward, 2014; Rehme, Eickhoff, et al., 2011; Volz, Sarfeld, et al., 2015).

Second, we tested for an association between rsFC and trEC: If rsFC and trEC indeed reflected similar state-general aspects of information integration within the stroke-afflicted motor network, we would expect rsFC and trEC to be associated across patients. In particular, connections that typically exhibit stroke-induced alterations at rest and during task performance such as ipsilateral premotor–M1 and interhemispheric M1–M1 may show similar changes and may thus be associated across patients. Finally, aiming to disentangle whether differences between rsFC and trEC can be ascribed to the activation state (task vs. rest) or the connectivity mode (functional vs. effective), we additionally computed task-related functional connectivity (trFC). If motor network changes observed after stroke were primarily driven by the activity state of the brain, we would expect trFC and trEC to be associated across patients. Alternatively, if connectivity estimates were rather mode-dependent than state-dependent, that is, assuming that the methodological approach used to compute connectivity heavily impacted our observations, one would expect to find a correlation between trFC and rsFC. Besides further elucidating the clinical potential of fMRI-based motor network connectivity estimates as biomarkers reflecting motor impairment, our findings help to more accurately interpret the commonly observed changes in rsFC and trEC after stroke.

2 | METHODS

2.1 | Data set

fMRI data analyzed here were initially obtained to assess the longitudinal effect of repeated intermittent theta-burst-stimulation (iTBS) on

the recovery of hand function and motor network reorganization (Volz et al., 2016). To rule out any confounding effects of the iTBS-intervention, we here only analyzed data obtained at baseline, that is, before iTBS was applied.

2.2 | Participants

Twenty-six first-ever ischemic stroke patients (mean age = 67 years, *SD* = 13, 9 females, 22 right-handed) were recruited from the University Hospital of Cologne, Department of Neurology (see Table S1 for demographic and lesion information). Inclusion criteria comprised age between 40 and 90 years, ischemic stroke as verified by diffusion-weighted magnetic resonance imaging (DWI) with a symptom onset within the past 2 weeks (average: 7.3 days ±3.6, one patient was included 16 days after stroke), unilateral hand motor impairment, no lesions affecting M1 hand representation or other cortical areas used in the network analysis, no severe aphasia, apraxia, or neglect, no visual field deficits or other neurological disorders. Exclusion criteria were defined as any contraindications to transcranial magnetic stimulation or MRI, infarcts in multiple territories, and hemorrhagic stroke. The study was carried out under the Declaration of Helsinki and had been approved by the local ethics committee of the University of Cologne. All subjects provided informed consent.

2.3 | Data acquisition

Participants underwent fMRI scans consisting of a resting-state sequence of 7 min and the subsequent performance of an active motor task. During the motor task, participants performed 20 blocks of unimanual rhythmically paced fist-closures. Each block lasted for 15 s, interrupted by breaks of 15 s (plus a temporal jitter of 1–2.5 s). Left- or right-hand-use was randomized across blocks.

Motor performance was assessed on the day of the fMRI scan using three different behavioral measures. First, as a robust parameter of basal hand motor performance, relative grip strength was determined as the ratio between the maximum grip strength of the affected and unaffected hand. We further included the Jebsen Taylor Test of Hand Function (JTT, Jebsen, Taylor, Trieschmann, Trotter, & Howard, 1969) and the Action Research Arm Test (ARAT, Lyle, 1981) as representations of more complex upper limb motor skills. For the JTT, each subtest was timed with a maximum time limit of 120 s, which was also assigned in case a subtask could not be performed (Duncan et al., 1998). In line with previous work (Rehme, Fink, von Cramon, & Grefkes, 2011), we computed a composite motor score by extracting the first principal component from a principal component analysis (PCA) comprising relative grip strength, ARAT, and JTT scores (explained variance by the first component = 90.95%), resulting in a measure that generalizes across different aspects of hand motor function with higher motor scores reflecting better performance.

fMRI data were recorded using a Siemens Trio 3.0 Tesla scanner (Siemens Medical Solutions, Erlangen, Germany). Resting-state images were acquired using a gradient-echo-planar (EPI) imaging sequence with the following parameters: repetition time (TR) = 2,200 ms, echo time (TE) = 30 ms, field of view (FOV) = 200 mm, 33 slices, voxel size: $3.1 \times 3.1 \times 3.1\ mm^3$, 20% distance factor, flip angle = 90°, 184 volumes. EPI volumes during the motor task were recorded using the same parameters for a total of 283 volumes. The slices covered the whole brain extending from the vertex to lower parts of the cerebellum. DWI were recorded to determine the localization and extent of acute stroke lesions (TR = 5,100 ms, TE = 104 ms, FOV = 230 mm, 30 slices, voxel size = $1.8 \times 1.8 \times 3.0\ mm^3$).

2.4 | Processing of fMRI data

Preprocessing of all fMRI-sequences was carried out using Statistical Parametric Mapping (SPM, The Wellcome Centre for Human Neuroimaging, London, UK, http://www.fil.ion.ucl.ac.uk/). Scans of six patients with right-hemispheric lesions were flipped along the mid-sagittal plane to ensure that all lesions were consistently located in the left hemisphere. The first four EPIs of each session were discarded as dummy images. The remaining volumes were realigned to the mean image of each time series. Based on the DWI showing the greatest lesion extent, we created lesion masks using MRIcron (www.sph.sc.edu/comd/rorden/MRicron), which were applied to the functional images. The DWI and lesion masks were co-registered with the realigned EPI images. Spatial normalization to the standard template of the Montreal Neurological Institute (MNI) was achieved through unified segmentation (Ashburner & Friston, 2005). Images were spatially smoothed using an isotropic Gaussian kernel of 8 mm full-width-at-half-maximum (FWHM).

Smoothed EPIs of the fMRI motor task time series were temporally high-pass filtered at 1/128 s. For the first-level analysis, a general linear model (GLM) using box-car vectors for the three experimental conditions (affected hand movement, unaffected hand movement, visual instructions) convolved with a canonical hemodynamic response function was used. Realignment parameters were included as covariates to reduce movement-related variance. For the second-level analysis, the first-level parameter estimates of the conditions "movement of the affected hand" and "movement of the unaffected hand" were entered into a full-factorial design with the within-subject factor "hand" (levels: unaffected vs. affected). The significance threshold for voxel-wise activation was set to $T > 5.1$ ($p < .05$, family-wise error-corrected at the voxel-level).

While trying to keep the preprocessing of resting-state and task-based fMRI data as similar as possible, several methodological idiosyncrasies resulted in subtle differences between both approaches. To remove variance attributable to known confounds from the resting-state time series, we included the six head motion parameters, their squared values and their first-order derivatives, as well as the mean-centered global gray matter, white matter, and cerebrospinal fluid signal intensities per time point obtained by averaging across tissue-class-specific voxels and their squared values as confound regressors into the analysis (Power et al., 2014; Satterthwaite et al., 2013).

Of note, for our primary analyses we did not use PCA-denoising to minimize preprocessing differences of resting-state and task-related data. A temporal bandpass filter was applied, retaining only frequencies between 0.01 and 0.08 Hz (Biswal, Zerrin Yetkin, Haughton, & Hyde, 1995; Fox & Raichle, 2007). To probe for the robustness of our results, we repeated our analyses (a) with PCA-denoising, using the first five principal components extracted by means of a PCA as regressors and (b) without global signal regression (GSR).

2.5 | Estimation of task-related effective connectivity

The analysis of trEC was carried out using DCM as implemented in SPM 12 (SPM12, The Wellcome Centre for Human Neuroimaging, London, UK, http://www.fil.ion.ucl.ac.uk/). DCM treats the brain as a deterministic and dynamic system in which inputs, that is, experimental conditions, cause the system to enter a specific state, which hence generates a certain output, that is, the local blood-oxygen-level-dependent signal (Friston et al., 2003). The following bilinear differential state equation expresses state changes over time:

$$\frac{dz}{dt} = \left[A + \sum_{j=1}^{m} u_j B^{(j)}\right] z + Cu$$

Z represents the neuronal state the system is in, u stands for the experimental input, and A, B, and C are matrices containing the coupling parameters, that is, the rates of change in neuronal population activity that arise from synaptic influences (Stephan et al., 2010; Stephan & Friston, 2010). More specifically, matrix A contains the endogenous connectivity inherent to the system in the absence of external perturbations. Matrix B captures the state changes elicited by external inputs such as experimental conditions, while matrix C contains the corresponding extrinsic influences. Thus, in our case, there were two DCM-B-matrices, one capturing changes elicited by affected hand movements and the other capturing changes related to unaffected hand movements. Of note, DCM is a hypothesis-driven technique that relies on a priori assumptions about the relevant brain regions involved. As computational constraints limit the maximum number of regions, we focused on regions highlighted as essential for the motor recovery process after stroke: bilateral M1, supplementary motor area (SMA), and ventral premotor cortex (PMv) (Grefkes, Nowak, et al., 2008; Grefkes et al., 2010; Rehme, Eickhoff, et al., 2011).

For each region of interest (ROI), we extracted the first eigenvariate of the time series adjusted for effects of interest within a 10 mm sphere around the local activation maximum (see Table S2 for the subject-specific VOI coordinates). The regions were determined individually for each subject by superimposing the subject-specific activation maps showing the contrasts "movement of the unaffected hand vs. rest" for regions in the right hemisphere and "movement of the affected hand vs. rest" for regions in the left hemisphere on a corresponding T1-weighted image. In line with previous work, definition of local activation maxima was aided by anatomical landmarks (Rehme, Eickhoff, et al., 2011; Volz, Sarfeld, et al., 2015): M1 on the rostral wall of the central sulcus ("hand knob formation") (Yousry, 1997), SMA on the medial wall within the interhemispheric fissure between the paracentral lobule and the coronal plane running through the anterior commissure (Picard & Strick, 2001), and PMv near the inferior precentral gyrus and pars opercularis (Rizzolatti, Fogassi, & Gallese, 2002). Determining individual ROIs via the local activation maximum enabled us to rule out that ROIs fell into lesioned and therefore no longer functional brain areas.

We computed a total of 44 DCMs that differed concerning their task-related DCM-B matrix, while the fully connected endogenous DCM-A matrix remained constant (Rehme, Eickhoff, et al., 2011; Volz, Sarfeld, et al., 2015). Driving inputs were set on the premotor regions, that is, bilateral SMA and PMv, and the DCM-C matrix was designed accordingly. We generated 44 models differing in task-related connectivity structures (i.e., DCM-B matrix, cf. Figure S1), grouped into four model families differing in terms of lateralization and directionality: (a) nonlateralized/bidirectional, (b) lateralized/bidirectional, (c) non-lateralized/unidirectional, and (d) lateralized/bidirectional. Directionality specified whether M1 only received inputs (unidirectional) or whether there was a feedback onto premotor areas (bidirectional). Lateralization described whether connections targeting bilateral M1 were present in the DCM-B matrix for movements of each hand (nonlateralized) or whether only the M1 contralateral to the moving hand was assumed to interact with premotor areas (lateralized).

To determine the model with the best balance between model fit and generalizability ("winning model"), we performed a Bayesian Model Selection (BMS) random effects analysis across all 44 models (Stephan, Penny, Daunizeau, Moran, & Friston, 2009). Additionally, Bayesian Model Averaging (BMA) was carried out for the model family showing the highest family-wise exceedance probability, and the resulting estimates were entered into a BMS to determine the most suitable model family for the given data. Connections were tested for significance using one-sample *t*-tests ($p < .05$, false discovery rate (FDR)-corrected for multiple comparisons).

2.6 | Estimation of resting-state functional connectivity

rsFC was computed as seed-to-seed correlations between the same motor regions as included in the DCM analysis, using identical individual regional coordinates to allow for comparisons with interregional DCM coupling parameters (Rehme et al., 2013). We used the same approach as defined in the DCM analysis to extract the first eigenvariate within a 10 mm sphere around each seed voxel. Next, we computed Pearson correlations between the time series of all region pairs. The resulting correlation coefficients were Fisher's *Z*-transformed using the formula $Z = 1/2 * \ln([1+r]/[1-r]) = \operatorname{atanh}(r)$ (Biswal et al., 1995) and tested for significance through one-sample *t*-tests ($p < .05$, FDR-corrected).

2.7 | Estimation of task-related functional connectivity

We computed trFC as seed-to-seed correlations between all possible region pairs individually for each subject. Based on the same coordinates as defined in the DCM- and resting-state analyses, we extracted the first eigenvariate from the time series of each ROI recorded during movement of the affected hand. Pearson correlations were computed on a single-subject level and Fisher's *Z*-transformed (Biswal et al., 1995). Significance was tested across subjects through one-sample *t*-tests ($p < .05$, FDR-corrected).

2.8 | Explaining motor impairment through connectivity estimates

To assess the relationship between connectivity measures and behavioral performance, we computed Spearman rank correlations between measures of rsFC as well as trEC (i.e., coupling parameters of the DCM-B-affected as well as DCM-B-unaffected matrix) and the composite motor score, as well as the individual motor scores.

Next, we tested to which extent rsFC and trEC explained variance in behavioral performance. We, therefore, computed multiple linear backward regression models with elimination based on the Bayesian information criterion (BIC, $k = \log(n)$ with $n = 26$), using the composite motor score as the outcome variable and either rsFC or trEC measures as predictors. We chose to base the selection of model predictors on the BIC rather than the AIC as the BIC allowed us to account for the relatively small sample size. With respect to the connectivity measures, we decided to focus on connections that have been shown to play a major role in motor network reorganization post stroke, that is, connections between bilateral premotor areas and affected M1 as well as interhemispheric connectivity between bilateral M1. Ideally, one would start the backward elimination process with the same number of connectivity measures in the trEC as in the rsFC-model. However, as trEC is directional whereas rsFC is nondirectional, trEC is expressed by two values per region pair, while rsFC only provides one value per region pair. As a result, the trEC starting model automatically contains twice as many values as the rsFC model. In our case, this meant that we started with one model with 10 trEC-coupling parameters and a second model with five rsFC-*z*-values. To ensure that a potential superiority of the trEC-based model was not merely driven by the difference in dimensionality, we repeated the rsFC-backward regression using a starting model with all 15 rsFC-measures. Moreover, to fully capture the potential of the trEC-based model given its higher granularity and number of connectivity estimates, we computed a trEC-based stepwise backward regression starting with all coupling parameters linked to either of the two M1. To minimize the likelihood of overfitting, model performance was compared via BIC values, penalizing model complexity.

Of note, using backward regression models for a comparison of different connectivity methods has two significant limitations: First, potential multicollinearity of predictor variables may render inference about the influence of individual connections difficult. Second, as described above, the fact that trEC is directional while rsFC is nondirectional results in a higher number of trEC measures, that is, a higher number of predictors for the corresponding starting model, hindering an unbiased comparison of the explanatory power of rsFC and trEC. To circumvent these limitations, we performed dimensionality reduction for rsFC and trEC by means of PCA, thereby translating measures of both connectivity types into an equal amount of meaningful, independent components. Three separate PCAs were calculated for rsFC as well as trEC, representing (a) ipsilesional, (b) contralesional, and (c) interhemispheric connections separately for rsFC and trEC (cf. Figure 1). Next, the estimated factor scores of the first principal components were used as predictors in the multiple linear regression models. First, each component was entered separately as a predictor to assess how much variance could be explained by each component individually. In other words, we computed three separate simple linear regressions for the rsFC-components and another three for the trEC-components. In a next step, multiple linear regression models were estimated, including the three first principal components of rsFC or trEC, respectively.

2.9 | Association of functional and effective connectivity

We assessed the relationship of rsFC, trEC, and trFC by computing Spearman rank correlations between the three DCM-matrices, the resting-state *Z*-values and the task-related *Z*-values for corresponding region pairs. We primarily used coupling parameters of the fully connected DCM-model as its B-matrix contains all connections present in the resting-state network. To ensure the reliability of our findings, we repeated the correlation analysis using (a) the winning model of the BMS, (b) the BMA results of the winning family, as well as resting-state *Z*-values obtained (c) without GSR and (d) with PCA-denoising. We assessed the significance of the resulting correlation coefficients by performing one-sample *t*-tests ($p < .05$, FDR-corrected).

3 | RESULTS

3.1 | Group-level motor network connectivity

Significant rsFC and trEC group-level averages are shown in Figure 2 and Figure S2. On the group-level, almost all rsFC connections reached statistical significance, resulting in a densely connected resting-state motor network (Figure 2a). DCM group results revealed facilitatory influences from bilateral premotor areas onto the ipsilesional M1 and inhibition from ipsilesional M1 onto premotor areas (Figure 2b) during movements of the paretic hand in line with previous findings (Diekhoff-Krebs et al., 2017; Rehme, Eickhoff, et al., 2011).

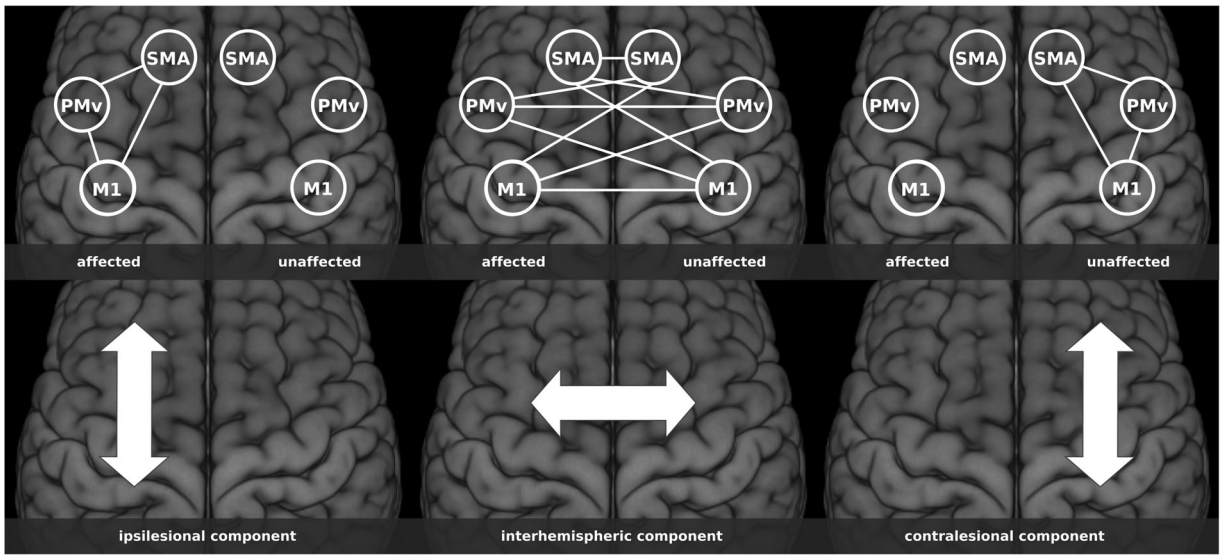

FIGURE 1 Principal components derived via PCA. The figure shows all connections that were summarized via PCAs. For the ipsilesional component, we used all connections between M1, SMA and PMv within the affected hemisphere, that is, three measures in case of rsFC and six measures in case of trEC. The interhemispheric component was derived from all interhemispheric connections, that is, from 9 measures in case of rsFC and 18 in case of trEC. For the contralesional component, all connections between M1, SMA and PMv within the unaffected hemisphere were used, that is, three measures in case of rsFC and six in case of trEC. DCM, dynamic causal modeling; PCA, principal component analysis; PMv, ventral premotor cortex; rsFC, resting-state functional connectivity; SMA, supplementary motor area; trEC, task-related effective connectivity

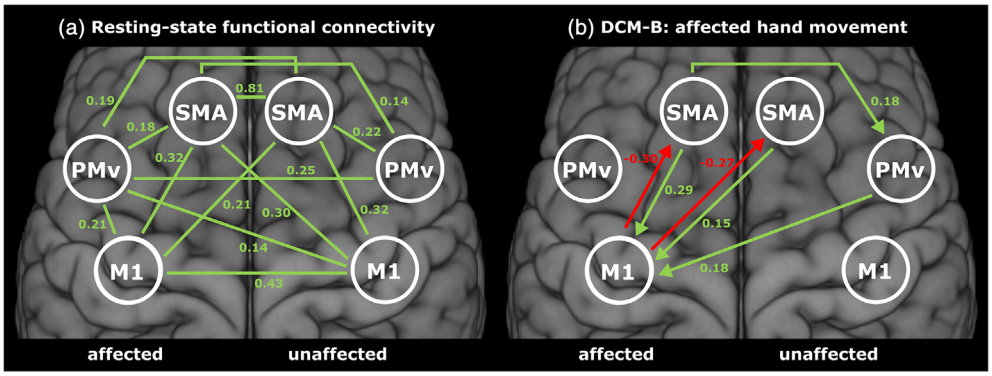

FIGURE 2 Group-level connectivity. Significant connections of the (a) resting-state *Z*-values and (b) DCM-coupling parameters during movement of the affected hand (DCM-B-affected matrix of the fully connected model), $p < .05$, FDR-corrected for multiple comparisons. The displayed values are group-level averages across patients. Missing connections between the displayed cortical regions did not reach significance after FDR-correction. DCM, dynamic causal modeling

3.2 | Motor impairment and connectivity: Correlation analyses

To address whether specific connections were indicative of motor performance after stroke, Spearman rank correlations were computed to probe for a relationship between the composite motor score with resting-state *Z*-values as well as coupling parameters modulated during hand movements of the affected or unaffected hand. No significant correlations were observed between rsFC or trEC and motor impairment ($p > .1$, FDR-corrected). Of note, highly similar results were obtained when repeating these analyses using individual behavioral scores (relative grip strength, ARAT, and JTT scores) rather than the composite motor score.

3.3 | Motor impairment and connectivity: Multiple linear backward regression

As single rsFC or trEC connections were not indicative of motor impairment across patients, multiple linear backward regression models were used to combine information from various connections across the motor network. Regression models obtained through

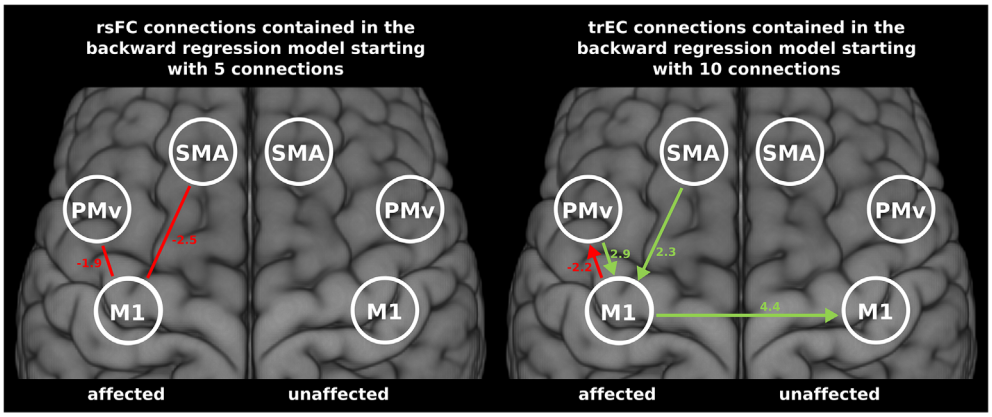

FIGURE 3 Results of the stepwise backward regression. Connections included in the resulting models are displayed with corresponding weights. Both models were able to explain behavioral variance as indicated by the overall model significance (rsFC-based regression model: $R^2 = 33.49\%$, adjusted $R^2 = 27.71\%$, $p = .009$, BIC = 24.25; trEC-based regression model: $R^2 = 55.41\%$, adjusted $R^2 = 46.92\%$, $p = .001$, BIC = 20.37). The connections that remain after backwards elimination are mostly ipsilesional premotor–M1 connections and the interhemispheric M1–M1 connection in case of trEC. rsFC, resting-state functional connectivity; trEC, task-related effective connectivity

stepwise backward elimination (starting with all premotor–M1 and the interhemispheric M1–M1 connection, that is, 10 trEC or 5 rsFC-measures) reached statistical significance for both rsFC and trEC ($p < .05$; see Figure 3). Specifically, the rsFC-model yielded 33.49% explained variance ($p = .009$, adjusted $R^2 = 27.71\%$, BIC = 24.25), while the trEC-based model explained 55.41% ($p = .001$, adjusted $R^2 = 46.92\%$, BIC = 20.37). Interestingly, the final rsFC-model contained only two ipsilesional premotor–M1 connections, highlighting the role of premotor–M1 connectivity within the affected hemisphere (see Equation (1)) early after stroke. While those connections were also included in the resulting trEC-model, it further comprised the interhemispheric M1–M1 connection (see Equation (2)). These findings are well in line with previous findings that stress the importance of those connections for stroke recovery.

$$Motor\ score = -2.5\,M1a - SMAa - 1.9\,M1a - PMva + 1.2 \quad (1)$$

$$Motor\ score = -2.2\,M1a - PMva + 2.3\,SMAa - M1a + 2.9\,PMva - M1a + 4.4\,M1a - M1u - 1.2 \quad (2)$$

Given the higher adjusted R^2 as well as the lower BIC-value of the final trEC-based model compared to the rsFC-based model, it seems like trEC may be more indicative of motor impairment than resting-state connectivity. To rule out that this finding was driven by the higher number of connectivity measures in the trEC-starting model (10 for trEC vs. 5 for rsFC), we computed an additional backward regression containing all 15 rsFC-measures in the initial model. The resulting model explained 62.67% of behavioral variance ($p = .006$), thereby outperforming the trEC-based model. However, when adjusting for the number of connections in the final model, it performed on a similar level as the trEC-based model according to the adjusted R^2-value of 48.14% while featuring a higher, that is, worse, BIC (BIC = 25.52). Last, to better capture the full potential of trEC, we computed a trEC-based backward regression starting with 18 connections that yielded an explained variance of 82.25% ($p < .001$, adjusted $R^2 = 70.42\%$, BIC = 15.97).

In summary, multiple linear backward regression models significantly explained variance in motor impairment across patients for both rsFC and trEC. While for rsFC premotor–M1 connections within the affected hemisphere were sufficient, trEC premotor–M1 coupling parameters and interhemispheric connectivity between bilateral M1 were needed to explain motor impairment.

3.4 | Dimensionality reduction via PCA: Regression results

As highlighted by the backward regression results, a direct comparison between trEC and trFC is hindered by a differing number of connectivity measures per region pair. Thus, we condensed trEC and rsFC into three components each (cf. Figure 1), reflecting ipsilesional, contralesional, and interhemispheric connectivity by performing dimensionality reduction via PCA. The six resulting principal components were entered into linear regression models to explain the composite motor score (see Figure 4 for the explained variance of the individual components). Significant results were exclusively obtained for components derived from rsFC scores: While the principal component of the ipsilesional rsFC values reached 26.98% explained variance ($p = .007$), the interhemispheric component accounted for 21.32% when entered individually into the regression model ($p = .018$). The remaining components did not result in significant regression models. Concerning the overall model including all three principal components, rsFC scores explained 29.35% of variance ($p = .050$), while the model based on trEC did not reach significance. In other words, for rsFC, ipsilesional premotor–M1 connectivity and interhemispheric connectivity could be aggregated to explain motor impairment, while trEC of each category did not sufficiently explain behavioral variance across patients.

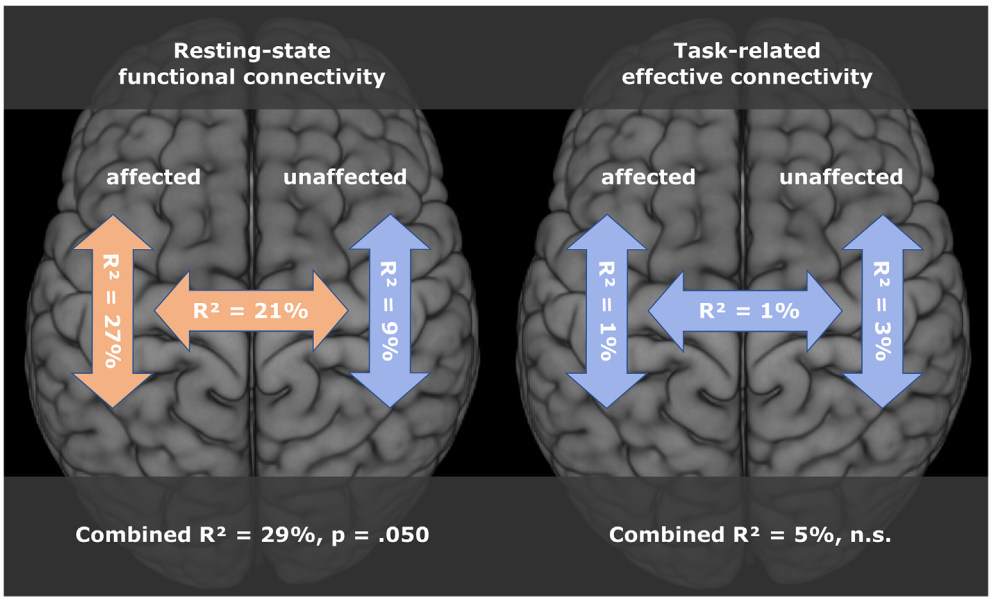

FIGURE 4 Explained motor impairment by individual PCA components. Values within the arrows indicate how much behavioral variance was explained when entering just the respective component into a regression model to predict motor performance. Orange arrows indicate a significant model; blue arrows indicate non-significance (significance threshold: $p < .05$). The combined R^2 denotes explanation of variance when entering all three components simultaneously into a regression model. Hence, the first principal component derived from the three ipsilesional rsFC-measures, as well as the first principal component derived from interhemispheric rsFC-measures significantly explained motor impairment. In general, regression models with PCA components based on resting-state connectivity yielded better results than PCA components based on DCM-coupling parameters, which failed to reach significance. DCM, dynamic causal modeling; PCA, principal component analysis; rsFC, resting-state functional connectivity

3.5 | Comparison of functional and effective connectivity

DCM parameters and resting-state *Z*-values of the cortical motor network were not significantly correlated (cf. Figure 5). To exclude that this result stemmed from using the fully connected DCM model or a specific resting-state preprocessing approach, we repeated the correlation analyses for (a) the winning model of the BMS, (b) average connection parameters obtained from the BMA procedure of the winning model family (i.e., Family 1), and resting-state *Z*-values obtained (c) with PCA-denoising and (d) without GSR. For all of these analyses, no significant correlations were observed between trEC and rsFC except for the interhemispheric M1a–PMvu connection, which showed an association between rsFC and trEC values of the DCM-A matrix when using resting-state *Z*-values obtained without GSR (cf. Figure S3 for correlations of the alternative models).

rsFC and trFC showed significant correlations for the interhemispheric connections of homolog region pairs, while no significant correlations were observed for trFC and trEC (cf. Figure 5, Figure S4). Thus, these results are in line with a mode-dependence of similarity in connectivity after stroke.

4 | DISCUSSION

In the present study, we conducted the first direct comparison of motor network rsFC and trEC in the early subacute stage after stroke. In line with our hypothesis, trEC was superior in explaining variance in motor performance when capitalizing on its richer informational complexity (i.e., higher number of connections) compared to rsFC. However, when balancing model complexity (i.e., using a similar number of connections), both frameworks explained motor impairment to a similar degree across patients. In line with previous findings, a combination of ipsilesional premotor–M1 connections and interhemispheric M1–M1 connectivity explained behavioral variance. As trEC and rsFC were unrelated for intrahemispheric as well as most interhemispheric connections, our findings suggest that rsFC and trEC reflect distinct aspects of information integration in the lesioned motor network after stroke, potentially hinting at distinct roles in motor network reorganization. Moreover, the significant associations observed between interhemispheric trFC and rsFC suggest that interhemispheric information integration after stroke might occur in a state-independent fashion, while ipsilesional premotor–M1 connectivity post-stroke seems to be state-dependent. Thus, our findings suggest two distinct aspects of functional network reorganization: (a) task-specific compensation via premotor–M1 in the ipsilesional hemisphere and (b) a more fundamental (i.e., task-independent) change in the interhemispheric interaction of motor homologs.

4.1 | Explaining motor impairment via resting-state vs. task-related connectivity

Both trEC and rsFC significantly explained motor performance, stressing the relevance of functional data as an indicator of motor

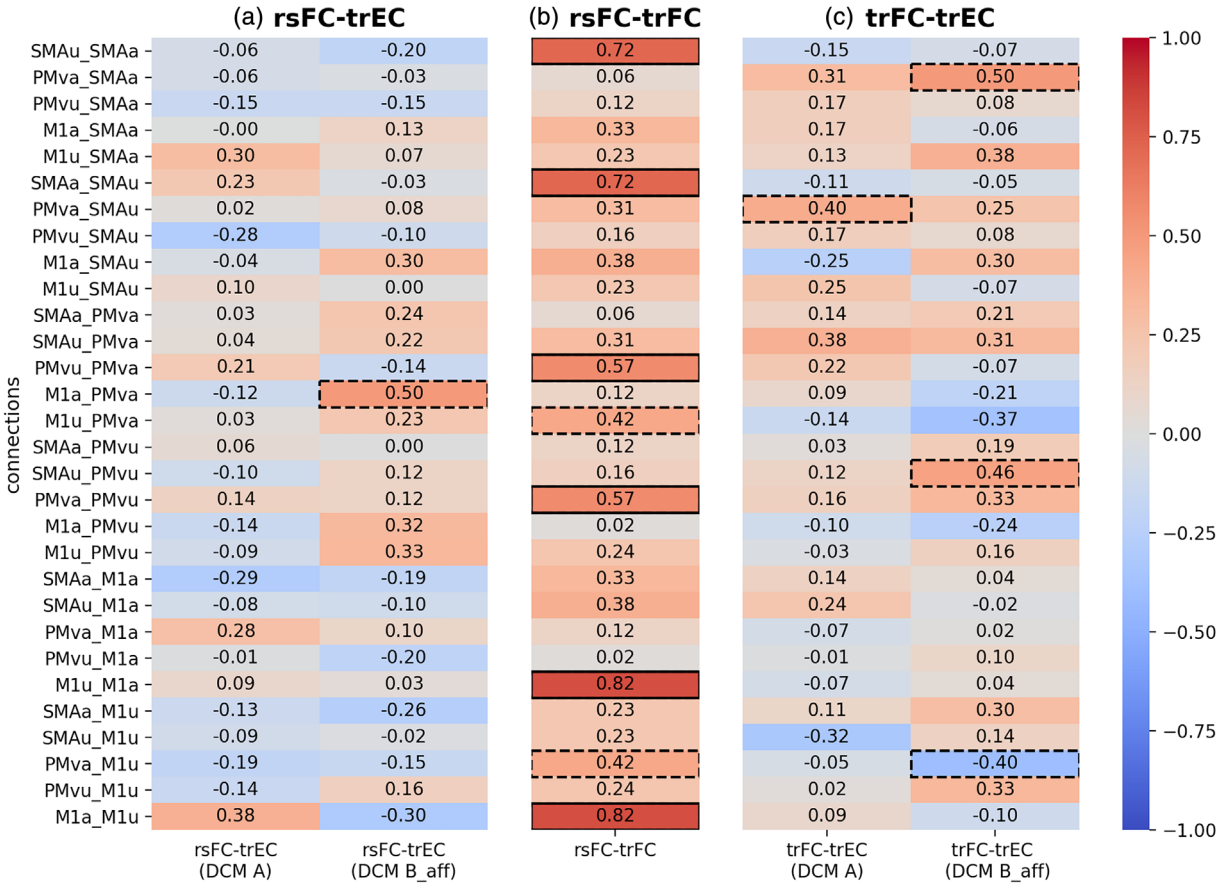

FIGURE 5 Spearman rank correlations between trEC, rsFC, and trFC. The three charts entail correlations between (a) rsFC and trEC, (b) rsFC and trFC, and (c) trFC and trEC. trEC is expressed in terms of coupling parameters of the DCM-A and B-affected matrix. rsFC is expressed as Fisher's *Z*-scores derived from Pearson correlations of the predefined region pairs. trFC was computed from the time series recorded during movement of the affected hand as Fisher's *Z*-scores derived from Pearson correlations of the predefined region pairs. Dashed lines indicate significance at an uncorrected level ($p < .05$), solid lines indicate significance after FDR-correction for multiple comparisons ($p < .05$, FDR-corrected). Of note, only rsFC and trFC (depicted in b) showed a significant relationship between interhemispheric homologous connections at a corrected level, suggesting a similarity in functional connectivity during task and rest, that is, depending on the connectivity mode and independent from the brain state. As FC is derived from a purely correlational approach, it is undirected and therefore contains only half as many connections as EC. In other words, while EC differentiates between for instance M1a–M1u and M1u–M1a connectivity, those values are the same for FC. Therefore, in the middle column (b) showing Spearman rank correlations between rsFC and trFC each correlation coefficient is displayed twice. DCM, dynamic causal modeling; FC, functional connectivity; rsFC, resting-state functional connectivity; trEC, task-related effective connectivity

impairment, well in line with previous studies (Baldassarre et al., 2016; Carter et al., 2009; Rehme, Volz, Feis, Eickhoff, et al., 2015; Rehme, Volz, Feis, Bomilcar-Focke, et al., 2015; van Meer et al., 2010; Volz, Sarfeld, et al., 2015). Directly comparing the propensity of rsFC and trEC to explain variance in motor impairment, the trEC-based regression model yielded higher explained variance and superior model evidence, as reflected by BIC (cf. Figure 3). However, the considerable difference in model complexity arising from the distinct number of rsFC and trEC connections renders a direct comparison of both models difficult. Accordingly, when including all rsFC connections and thus increasing their number above the number of trEC connections, the rsFC-based model somewhat surprisingly explained behavioral variance to a similar extent compared to the trEC-based model, yet at the cost of increased model complexity as indicated by a higher number of connections in the resulting regression model as well as an increased BIC-value.

In summary, when utilizing the higher degree of information contained in trEC, that is, the higher number of connections due to its directionality, it outperformed rsFC in explaining variance of motor performance, in line with our initial hypothesis. However, trEC results are less likely to generalize, given their strong task-dependence and the propensity of more complex statistical models to more easily over-fit the data at hand. When reducing the number of connectivity estimates to enable a more even comparison, rsFC and trEC both significantly explained motor performance to a rather similar degree. Therefore, our results highlight the potential role of both rsFC and trEC as potential biomarkers for motor impairment. Given its superior feasibility in a clinical context, our current findings particularly emphasize the clinical potential of rsFC.

4.2 | Task-related motor network connectivity after stroke

After the advent of fMRI, various studies have conclusively reported increased BOLD-activity levels during paretic hand movements in both the ipsi- and contralesional hemisphere (Rehme, Eickhoff, Rottschy, Fink, & Grefkes, 2012). trEC has often been used to further elucidate the mechanistic underpinnings of such altered activity patterns from a network level-perspective (Grefkes & Fink, 2014). A common finding replicated across studies analyzing trEC in stroke patients highlights the crucial role of excitatory ipsilesional premotor–M1 coupling which is thought to enable movements by driving M1 activity necessary to activate muscles via descending motor activity (Grefkes, Nowak, et al., 2008; Grefkes et al., 2010; Hensel et al., 2021; Rehme, Eickhoff, et al., 2011). In line with this notion, our current analysis implies that stronger excitatory coupling from ipsilesional premotor areas onto the affected M1 as well as stronger inhibitory feedback from the affected M1 back onto the ipsilesional PMv were indicative of better motor performance (cf. Figure 3). Thus, our current findings highlight the functional importance of excitatory premotor–M1 connectivity early after stroke.

Another recurrent, albeit more complex and variable finding lies in altered interhemispheric M1–M1 connectivity. In healthy subjects, unilateral hand movements have repetitively been shown to elicit an inhibitory influence from the *active* M1 (contralateral to the moving hand) onto the *inactive* M1 (ipsilateral to the moving hand; Grefkes, Nowak, et al., 2008; Pool et al., 2013; Pool, Rehme, Fink, Eickhoff, & Grefkes, 2014; Rehme, Eickhoff, et al., 2011; Volz, Hamada, Rothwell, & Grefkes, 2015; Volz, Sarfeld, et al., 2015). After stroke, distinct alterations of M1–M1 trEC have been reported presumably depending on the time-point post stroke and severity of motor impairment, ranging from a lack of inhibition of contralesional M1 by ipsilesional M1 to additional facilitatory influence from the unaffected M1 onto the affected M1 (Hensel et al., 2021; Rehme, Eickhoff, et al., 2011). Accordingly, our present findings also emphasize that interhemispheric M1–M1 connectivity is functionally relevant after stroke. Specifically, stronger excitatory influences from ipsilesional M1 onto contralesional M1 were indicative for better motor performance. From a conceptual perspective, this result may represent a mechanism of task-specific compensation. Mechanistically, pronounced excitation of the contralesional M1 by the ipsilesional would lead to increased activation of the contralesional M1 during paretic hand movements. This finding is well in line with the *vicariation model* (Di Pino et al., 2014), ascribing a supportive role to the over-activation of the contralesional M1 during motor task performance with the paretic hand, as argued by various previous studies (Rehme, Fink, et al., 2011; Tombari et al., 2004; Ward, Brown, Thompson, & Frackowiak, 2003). A similar supportive role of the ipsilateral M1 has also been observed in healthy subjects for complex motor tasks, giving rise to the notion that additional ipsilateral (i.e., contralesional in stroke patients) resources are activated with increased task demands (Verstynen, Diedrichsen, Albert, Aparicio, & Ivry, 2005).

However, the functional role of the contralesional M1 for motor performance of the paretic hand ultimately remains controversial, with evidence from several studies suggesting a maladaptive role of the contralesional M1 (Grefkes et al., 2010; Grefkes, Nowak, et al., 2008; Murase, Duque, Mazzocchio, & Cohen, 2004; Volz et al., 2017; Volz, Sarfeld, et al., 2015). A reason for these diverging findings and interpretations may lie in their dependence on the motor task performed in a given study (Hartwigsen & Volz, 2021; Lotze et al., 2006; Volz et al., 2017). Specifically, stroke patients typically develop individual compensation strategies to master a given movement impacting on trEC. Thus, such specific compensatory efforts of the lesioned motor system might therefore comprise highly individual changes that are less easily captured on the group level. In other words, idiosyncratic patterns of trEC changes may be present in distinct subjects that do not generalize well to the group level.

4.3 | Task-independent motor network connectivity after stroke

By contrast, rsFC offers the opportunity to assess the motor network in a task-independent fashion, allowing for easier generalization of findings and clinical application. After stroke, characteristic changes in rsFC have convergingly been reported across different studies, highlighting a crucial role of interhemispheric M1–M1 connectivity, which has been shown to first decrease and then re-increase alongside functional recovery in both humans and animal models (for references regarding interhemispheric changes, see, e.g., Carter et al., 2009; Golestani et al., 2013; van Meer et al., 2010, 2012). While we did not observe a significant correlation between M1–M1 rsFC-connectivity and motor performance in our current study, variance in motor impairment was significantly explained when entering the first principal component derived from all interhemispheric rsFC-connections into a regression model (cf. Figure 4). In other words, combining interhemispheric connections significantly explained motor impairment, stressing the importance of premotor areas beyond interhemispheric M1–M1 connectivity in rsFC early after stroke. Besides interhemispheric connections, ipsilesional premotor–M1 connectivity also played a major role: regression weights indicated a negative relationship between motor performance and ipsilesional SMA–M1 as well as PMv–M1 connection strength (cf. Figure 3). Moreover, the regression model containing the ipsilesional PCA-component achieved the highest explained variance. While reported less frequently than altered M1–M1 connectivity, previous studies have already outlined the functional significance of premotor–M1 rsFC after stroke. For example, Carter et al. found that interhemispheric rsFC alone was not significantly related to behavioral impairment, yet it explained motor impairment when complemented by intrahemispheric rsFC and lesion size (Carter et al., 2012). Furthermore, Rehme and colleagues reported their machine learning classification to be partially driven by increased connectivity between ipsilesional premotor areas and the affected M1 (Rehme, Volz, Feis, Bomilcar-Focke, et al., 2015). Of note, this evidence supporting a negative relationship between rsFC and motor

performance post-stroke is challenged by data observing the opposite relationship. For instance, a study investigating rsFC in patients within the first 2 weeks post-stroke found a positive association between ipsilesional PMv–M1 connectivity in the acute phase and motor improvement over the course of the next 3 months for a subgroup of severely affected patients (Lee et al., 2017). For the chronic stage, there are also reports of a positive link between premotor–M1 rsFC and motor function (Lam et al., 2018). Thus, the association of altered ipsilesional rsFC post-stroke with motor impairment seems to vary depending on the analytic framework, degree of motor impairment as well as the time since stroke included in a specific study.

In summary, premotor–M1-rsFC within the ipsilesional hemisphere seems to play a crucial role after stroke and should not be neglected next to the commonly reported interhemispheric connectivity changes (Carter et al., 2009; Golestani et al., 2013; van Meer et al., 2010, 2012).

4.4 | Task-specific ipsilesional compensation and general interhemispheric reorganization

We here showed for the first time that ipsilesional and interhemispheric components of both rsFC and trEC readily explained motor impairment post-stroke in the same cohort of patients, while replicating previous findings obtained for either rsFC or trEC in isolation. The observed overlap of explanatory components between rsFC and trEC emphasizes the question whether both similarly capture fundamental aspects of motor network reorganization in a task-independent fashion. Conversely, findings obtained from healthy human subjects support the notion that rsFC and trEC rather reflect differential, state-independent aspects of information integration (Rehme et al., 2013). Our current results revealed a similar lack of overlap between trEC and rsFC in the early phase post-stroke (cf. Figure 5). Thus, despite the fact that stroke-induced changes in motor network connectivity affect highly similar connections, rsFC and trEC seem to reflect largely unrelated aspects of information integration. However, the fact that we observed significant correlations between trFC and rsFC-measures of homologous interhemispheric connections indicates a state-independent similarity of interhemispheric connectivity after stroke (cf. Figure 5). In light of these results, the lack of a relationship between interhemispheric rsFC and trEC seems to depend on the mode, that is, to result at least in part from the methodological approach used to calculate connectivity, rather than the activity state of the brain. In other words, functional connectivity between interhemispheric homologs seems to reflect similar neural interactions post-stroke irrespective of whether the motor system is engaged in task execution or at rest. Taken together, task-independent changes of interhemispheric connectivity may result from a general, task-independent aspect of motor network reorganization. One might speculate that recruiting the computational resources of the functional homolog in the other hemisphere may be a highly efficient and domain-general way of functionally extending the lesioned network by using the pre-existing prominent structural connections via the corpus callosum allowing for direct information exchange. Support for the notion that involving bilateral functional homologs in the attempt to compensate for tissue loss may be a highly general mechanism derives from the fact that changes in interhemispheric activation and connectivity have been observed in multiple functional systems such as the motor, language and cognitive networks both at rest and during task-performance (Hartwigsen & Volz, 2021).

Conversely, while we found that premotor–M1 connectivity onto ipsilesional M1 crucially contributed to the explanation of motor impairment for both rsFC and trEC, the lack of association between rsFC and trFC suggests that premotor-M1 connectivity may indeed be highly state-dependent. From a mechanistic perspective, this does not seem surprising, given the pivotal role of premotor–M1 connections for the production of voluntary actions such as grasping or reaching movements (Cunnington, Bradshaw, & Iansek, 1996; Davare, 2006; Davare, Lemon, & Olivier, 2008; Kazennikov et al., 1999; Rizzolatti et al., 2002). Conceptually, one might thus assume that the state-dependence of ipsilesional premotor–M1 connectivity reflects the network's attempt to maximize its functionality to serve the specific task at hand. In sum, premotor–M1 connectivity may thus be attributed to task-specific compensation, while interhemispheric connectivity seems to change in a task-independent fashion, potentially reflecting a general aspect of motor network reorganization.

4.5 | Limitations

We here compared the two most commonly used methodological approaches to estimate connectivity from fMRI data in stroke patients. Importantly, while we included trFC to differentiate between state- and mode-specific effects, we refrained from adding resting-state effective connectivity (rsEC) to our analyses. Even though some efforts have been made to estimate effective connectivity from resting-state data using DCM-based approaches (Friston, Kahan, Biswal, & Razi, 2014; Friston, Li, Daunizeau, & Stephan, 2011; Li et al., 2011; Razi, Kahan, Rees, & Friston, 2015), such an approach has to the best of our knowledge never been applied in stroke patients. While the assessment of rsEC after stroke certainly represents a highly interesting scientific question, the focus of the current study was to compare established methodological frameworks which have previously reported similar motor network alterations after stroke. Thus, the first assessment of DCM-based rsEC after stroke is beyond the scope of the current manuscript and should be addressed in future work.

Regression results are heavily influenced by methodological decisions so that the reported connections contributing to the explanation of motor impairment have to be interpreted with caution. For instance, with respect to the stepwise backward regression, other starting models might yield diverging results and other combinations of connectivity measures might achieve similar explanatory power as the ones reported here. An important parameter choice lies in the elimination criterion used in the stepwise backward regression. To account for the

high number of model parameters relative to our sample size we opted for BIC to protect against overfitting. Of note, repeating our analyses using AIC instead of BIC yielded slightly different surviving connections in the final regression model, yet a similar percentage of explained variance, corroborating the robustness of our findings.

Although we here investigated a significantly bigger sample than previous DCM-studies in stroke patients, the limited sample size does still not allow for conclusions regarding the heterogeneity in lesion location and size and the associated variability in reorganization processes. Future research should therefore attempt to recruit larger samples, including patients of the early acute or chronic stage and try to expand the present findings to other functional networks.

5 | CONCLUSION

Comparing trEC and rsFC in the first 2 weeks after stroke, using the superior complexity offered by trEC best explained variance in motor performance. However, when balancing model complexity, connectivity measures of both frameworks explained motor performance in the early subacute phase post-stroke to a similar extent, underscoring the clinical potential of rsFC given its superior feasibility and generalizability. For both approaches, connectivity between ipsilesional premotor–M1 as well as interhemispheric M1–M1 explained motor impairment early after stroke. Besides frequently observed alterations of interhemispheric M1–M1 connectivity, our findings thus particularly highlight the crucial role of premotor–M1 connectivity in early motor network reorganization. From a mechanistic perspective, premotor–M1 connectivity seems to primarily reflect state-dependent compensation, while state-independent interhemispheric connectivity between motor homologs may potentially arise from general aspects of functional motor network reorganization reflected during both task-performance and at rest.

ACKNOWLEDGMENTS

Anne K. Rehme is supported by the Deutsche Forschungsgemeinschaft (DFG, German Research Foundation, RE3014/2-1). Simon B. Eickhoff acknowledges funding through the European Union's Horizon 2020 Research and Innovation Program (grant agreements 785907 [HBP SGA2] and 945539 [HBP SGA3]). Gereon R. Fink and Christian Grefkes are funded by the Deutsche Forschungsgemeinschaft (DFG, German Research Foundation)—Project-ID 431549029—SFB 1451. Gereon R. Fink gratefully acknowledges additional support from the Marga and Walter Boll Stiftung. Open access funding enabled and organized by Projekt DEAL.

DATA AVAILABILITY STATEMENT

The data that support the findings of this study are available from the corresponding author upon reasonable request.

ORCID

Christian Grefkes https://orcid.org/0000-0002-1656-720X
Lukas J. Volz https://orcid.org/0000-0002-0161-654X

REFERENCES

Ashburner, J., & Friston, K. J. (2005). Unified segmentation. *NeuroImage*, *26*(3), 839–851. https://doi.org/10.1016/j.neuroimage.2005.02.018

Baldassarre, A., Ramsey, L., Rengachary, J., Zinn, K., Siegel, J. S., Metcalf, N. V., … Shulman, G. L. (2016). Dissociated functional connectivity profiles for motor and attention deficits in acute right-hemisphere stroke. *Brain*, *139*(7), 2024–2038. https://doi.org/10.1093/brain/aww107

Biswal, B., Zerrin Yetkin, F., Haughton, V. M., & Hyde, J. S. (1995). Functional connectivity in the motor cortex of resting human brain using echo-planar mri. *Magnetic Resonance in Medicine*, *34*(4), 537–541. https://doi.org/10.1002/mrm.1910340409

Buxton, R. B., Wong, E. C., & Frank, L. R. (1998). Dynamics of blood flow and oxygenation changes during brain activation: The ballon model. *Magnetic Resonance in Medicine*, *39*(17), 855–864. https://doi.org/10.1002/mrm.1910390602

Carter, A. R., Astafiev, S. V., Lang, C. E., Connor, L. T., Rengachary, J., Strube, M. J., … Corbetta, M. (2009). Resting state inter-hemispheric fMRI connectivity predicts performance after stroke. *Annals of Neurology*, *67*(3), 365–375. https://doi.org/10.1002/ana.21905

Carter, A. R., Patel, K. R., Astafiev, S. V., Snyder, A. Z., Rengachary, J., Strube, M. J., … Corbetta, M. (2012). Upstream dysfunction of Somatomotor functional connectivity after Corticospinal damage in stroke. *Neurorehabilitation and Neural Repair*, *26*(1), 7–19. https://doi.org/10.1177/1545968311411054

Cramer, S. C. (2008). Repairing the human brain after stroke: I. Mechanisms of spontaneous recovery. *Annals of Neurology*, *63*(3), 272–287. https://doi.org/10.1002/ana.21393

Cunnington, R., Bradshaw, J. L., & Iansek, R. (1996). The role of the supplementary motor area in the control of voluntary movement. *Human Movement Science*, *15*(5), 627–647. https://doi.org/10.1016/0167-9457(96)00018-8

Davare, M. (2006). Dissociating the role of ventral and dorsal premotor cortex in precision grasping. *Journal of Neuroscience*, *26*(8), 2260–2268. https://doi.org/10.1523/JNEUROSCI.3386-05.2006

Davare, M., Lemon, R., & Olivier, E. (2008). Selective modulation of interactions between ventral premotor cortex and primary motor cortex during precision grasping in humans. *Journal of Physiology*, *586*(11), 2735–2742. https://doi.org/10.1113/jphysiol.2008.152603

Di Pino, G., Pellegrino, G., Assenza, G., Capone, F., Ferreri, F., Formica, D., … Di Lazzaro, V. (2014). Modulation of brain plasticity in stroke: A novel model for neurorehabilitation. *Nature Reviews Neurology*, *10*(10), 597–608. https://doi.org/10.1038/nrneurol.2014.162

Diekhoff-Krebs, S., Pool, E. M., Sarfeld, A. S., Rehme, A. K., Eickhoff, S. B., Fink, G. R., & Grefkes, C. (2017). Interindividual differences in motor network connectivity and behavioral response to iTBS in stroke patients. *NeuroImage: Clinical*, *15*(June), 559–571. https://doi.org/10.1016/j.nicl.2017.06.006

Duncan, P., Richards, L., Wallace, D., Stoker-Yates, J., Pohl, P., Luchies, C., … Studenski, S. (1998). A randomized, controlled pilot study of a home-based exercise program for individuals with mild and moderate stroke. *Stroke*, *29*(10), 2055–2060. https://doi.org/10.1161/01.STR.29.10.2055

Fox, M. D., & Raichle, M. E. (2007). Spontaneous fluctuations in brain activity observed with functional magnetic resonance imaging. *Nature Reviews Neuroscience*, *8*(9), 700–711. https://doi.org/10.1038/nrn2201

Friston, K. J. (1994). Functional and effective connectivity in neuroimaging: A synthesis. *Human Brain Mapping*, *2*(1–2), 56–78. https://doi.org/10.1002/hbm.460020107

Friston, K. J., Harrison, L., & Penny, W. (2003). Dynamic causal modelling. *NeuroImage*, *19*(4), 1273–1302. https://doi.org/10.1016/S1053-8119(03)00202-7

Friston, K. J., Kahan, J., Biswal, B., & Razi, A. (2014). A DCM for resting state fMRI. *NeuroImage*, *94*, 396–407. https://doi.org/10.1016/j.neuroimage.2013.12.009

Friston, K. J., Li, B., Daunizeau, J., & Stephan, K. E. (2011). Network discovery with DCM. *NeuroImage*, *56*(3), 1202–1221. https://doi.org/10.1016/j.neuroimage.2010.12.039

Golestani, A.-M., Tymchuk, S., Demchuk, A., & Goodyear, B. G. (2013). Longitudinal evaluation of resting-state fMRI after acute stroke with hemiparesis. *Neurorehabilitation and Neural Repair*, *27*(2), 153–163. https://doi.org/10.1177/1545968312457827

Grefkes, C., Eickhoff, S. B., Nowak, D. A., Dafotakis, M., & Fink, G. R. (2008). Dynamic intra- and interhemispheric interactions during unilateral and bilateral hand movements assessed with fMRI and DCM. *NeuroImage*, *41*(4), 1382–1394. https://doi.org/10.1016/j.neuroimage.2008.03.048

Grefkes, C., & Fink, G. R. (2014). Connectivity-based approaches in stroke and recovery of function. *The Lancet Neurology*, *13*(2), 206–216. https://doi.org/10.1016/S1474-4422(13)70264-3

Grefkes, C., Nowak, D. A., Eickhoff, S. B., Dafotakis, M., Küst, J., Karbe, H., & Fink, G. R. (2008). Cortical connectivity after subcortical stroke assessed with functional magnetic resonance imaging. *Annals of Neurology*, *63*(2), 236–246. https://doi.org/10.1002/ana.21228

Grefkes, C., Nowak, D. A., Wang, L. E., Dafotakis, M., Eickhoff, S. B., & Fink, G. R. (2010). Modulating cortical connectivity in stroke patients by rTMS assessed with fMRI and dynamic causal modeling. *NeuroImage*, *50*(1), 233–242. https://doi.org/10.1016/j.neuroimage.2009.12.029

Grefkes, C., & Ward, N. S. (2014). Cortical reorganization after stroke. *The Neuroscientist*, *20*(1), 56–70. https://doi.org/10.1177/1073858413491147

Hartwigsen, G., & Volz, L. J. (2021). Probing rapid network reorganization of motor and language functions via neuromodulation and neuroimaging. *NeuroImage*, *224*(October 2020), 117449. https://doi.org/10.1016/j.neuroimage.2020.117449

Hensel, L., Tscherpel, C., Freytag, J., Ritter, S., Rehme, A. K., Volz, L. J., … Grefkes, C. (2021). Connectivity-related roles of Contralesional brain regions for motor performance early after stroke. *Cerebral Cortex*, *31*(2), 993–1007. https://doi.org/10.1093/cercor/bhaa270

Jebsen, R. H., Taylor, N., Trieschmann, R. B., Trotter, M. J., & Howard, L. A. (1969). An objective and standardized test of hand function. *Archives of Physical Medicine and Rehabilitation*, *50*(6), 311–319.

Kazennikov, O., Hyland, B., Corboz, M., Babalian, A., Rouiller, E. M., & Wiesendanger, M. (1999). Neural activity of supplementary and primary motor areas in monkeys and its relation to bimanual and unimanual movement sequences. *Neuroscience*, *89*(3), 661–674. https://doi.org/10.1016/S0306-4522(98)00348-0

Lam, T. K., Dawson, D. R., Honjo, K., Ross, B., Binns, M. A., Stuss, D. T., … Chen, J. L. J. (2018). Neural coupling between contralesional motor and frontoparietal networks correlates with motor ability in individuals with chronic stroke. *Journal of the Neurological Sciences*, *384*(November 2017), 21–29. https://doi.org/10.1016/j.jns.2017.11.007

Lee, J., Park, E., Lee, A., Chang, W. H., Kim, D. S., & Kim, Y. H. (2017). Recovery-related indicators of motor network plasticity according to impairment severity after stroke. *European Journal of Neurology*, *24*(10), 1290–1299. https://doi.org/10.1111/ene.13377

Li, B., Daunizeau, J., Stephan, K. E., Penny, W., Hu, D., & Friston, K. (2011). Generalised filtering and stochastic DCM for fMRI. *NeuroImage*, *58*(2), 442–457. https://doi.org/10.1016/j.neuroimage.2011.01.085

Lotze, M., Markert, J., Sauseng, P., Hoppe, J., Plewnia, C., & Gerloff, C. (2006). The role of multiple contralesional motor areas for complex hand movements after internal capsular lesion. *The Journal of Neuroscience: The Official Journal of the Society for Neuroscience*, *26*(22), 6096–6102. https://doi.org/10.1523/JNEUROSCI.4564-05.2006

Lyle, R. C. (1981). A performance test for assessment of upper limb function in physical rehabilitation treatment and research. *International Journal of Rehabilitation Research*, *4*(4), 483–492.

Murase, N., Duque, J., Mazzocchio, R., & Cohen, L. G. (2004). Influence of interhemispheric interactions on motor function in chronic stroke. *Annals of Neurology*, *55*(3), 400–409. https://doi.org/10.1002/ana.10848

Park, C. H., Chang, W. H., Ohn, S. H., Kim, S. T., Bang, O. Y., Pascual-Leone, A., & Kim, Y.-H. H. (2011). Longitudinal changes of resting-state functional connectivity during motor recovery after stroke. *Stroke*, *42*(5), 1357–1362. https://doi.org/10.1161/STROKEAHA.110.596155

Picard, N., & Strick, P. L. (2001). Imaging the premotor areas. *Current Opinion in Neurobiology*, *11*(6), 663–672. https://doi.org/10.1016/S0959-4388(01)00266-5

Pool, E.-M., Rehme, A. K., Fink, G. R., Eickhoff, S. B., & Grefkes, C. (2013). Network dynamics engaged in the modulation of motor behavior in healthy subjects. *NeuroImage*, *82*, 68–76. https://doi.org/10.1016/j.neuroimage.2013.05.123

Pool, E.-M., Rehme, A. K., Fink, G. R., Eickhoff, S. B., & Grefkes, C. (2014). Handedness and effective connectivity of the motor system. *NeuroImage*, *99*, 451–460. https://doi.org/10.1016/j.neuroimage.2014.05.048

Power, J. D., Mitra, A., Laumann, T. O., Snyder, A. Z., Schlaggar, B. L., & Petersen, S. E. (2014). Methods to detect, characterize, and remove motion artifact in resting state fMRI. *NeuroImage*, *84*, 320–341. https://doi.org/10.1016/j.neuroimage.2013.08.048

Razi, A., Kahan, J., Rees, G., & Friston, K. J. (2015). Construct validation of a DCM for resting state fMRI. *NeuroImage*, *106*, 1–14. https://doi.org/10.1016/j.neuroimage.2014.11.027

Rehme, A. K., Eickhoff, S. B., & Grefkes, C. (2013). State-dependent differences between functional and effective connectivity of the human cortical motor system. *NeuroImage*, *67*, 237–246. https://doi.org/10.1016/j.neuroimage.2012.11.027

Rehme, A. K., Eickhoff, S. B., Rottschy, C., Fink, G. R., & Grefkes, C. (2012). Activation likelihood estimation meta-analysis of motor-related neural activity after stroke. *NeuroImage*, *59*(3), 2771–2782. https://doi.org/10.1016/j.neuroimage.2011.10.023

Rehme, A. K., Eickhoff, S. B., Wang, L. E., Fink, G. R., & Grefkes, C. (2011). Dynamic causal modeling of cortical activity from the acute to the chronic stage after stroke. *NeuroImage*, *55*(3), 1147–1158. https://doi.org/10.1016/j.neuroimage.2011.01.014

Rehme, A. K., Fink, G. R., von Cramon, D. Y., & Grefkes, C. (2011). The role of the Contralesional motor cortex for motor recovery in the early days after stroke assessed with longitudinal fMRI. *Cerebral Cortex*, *21*(4), 756–768. https://doi.org/10.1093/cercor/bhq140

Rehme, A. K., Volz, L. J., Feis, D.-L., Bomilcar-Focke, I., Liebig, T., Eickhoff, S. B., … Grefkes, C. (2015). Identifying neuroimaging markers of motor disability in acute stroke by machine learning techniques. *Cerebral Cortex*, *25*(9), 3046–3056. https://doi.org/10.1093/cercor/bhu100

Rehme, A. K., Volz, L. J., Feis, D. L., Eickhoff, S. B., Fink, G. R., & Grefkes, C. (2015). Individual prediction of chronic motor outcome in the acute post-stroke stage: Behavioral parameters versus functional imaging. *Human Brain Mapping*, *36*(11), 4553–4565. https://doi.org/10.1002/hbm.22936

Rizzolatti, G., Fogassi, L., & Gallese, V. (2002). Motor and cognitive functions of the ventral premotor cortex. *Current Opinion in Neurobiology*, *12*(2), 149–154. https://doi.org/10.1016/S0959-4388(02)00308-2

Satterthwaite, T. D., Elliott, M. A., Gerraty, R. T., Ruparel, K., Loughead, J., Calkins, M. E., … Wolf, D. H. (2013). An improved framework for confound regression and filtering for control of motion artifact in the preprocessing of resting-state functional connectivity data. *NeuroImage*, *64*(1), 240–256. https://doi.org/10.1016/j.neuroimage.2012.08.052

Stephan, K. E., & Friston, K. J. (2010). Analyzing effective connectivity with functional magnetic resonance imaging. *Wiley Interdisciplinary Reviews: Cognitive Science*, *1*(3), 446–459. https://doi.org/10.1002/wcs.58

Stephan, K. E., Penny, W. D., Daunizeau, J., Moran, R. J., & Friston, K. J. (2009). Bayesian model selection for group studies. *NeuroImage*, *46*(4), 1004–1017. https://doi.org/10.1016/j.neuroimage.2009.03.025

Stephan, K. E., Penny, W. D., Moran, R. J., den Ouden, H. E. M., Daunizeau, J., & Friston, K. J. (2010). Ten simple rules for dynamic

causal modeling. *NeuroImage*, *49*(4), 3099–3109. https://doi.org/10.1016/j.neuroimage.2009.11.015

Thiel, A., & Vahdat, S. (2015). Structural and resting-state brain connectivity of motor networks after stroke. *Stroke*, *46*(1), 296–301. https://doi.org/10.1161/STROKEAHA.114.006307

Tombari, D., Loubinoux, I., Pariente, J., Gerdelat, A., Albucher, J.-F., Tardy, J., … Chollet, F. (2004). A longitudinal fMRI study: In recovering and then in clinically stable sub-cortical stroke patients. *NeuroImage*, *23*(3), 827–839. https://doi.org/10.1016/j.neuroimage.2004.07.058

van Meer, M. P. A., Otte, W. M., van der Marel, K., Nijboer, C. H., Kavelaars, A., van der Sprenkel, J. W. B., … Dijkhuizen, R. M. (2012). Extent of bilateral neuronal network reorganization and functional recovery in relation to stroke severity. *Journal of Neuroscience*, *32*(13), 4495–4507. https://doi.org/10.1523/JNEUROSCI.3662-11.2012

van Meer, M. P. A., van der Marel, K., Wang, K., Otte, W. M., el Bouazati, S., Roeling, T. A. P., … Dijkhuizen, R. M. (2010). Recovery of sensorimotor function after experimental stroke correlates with restoration of resting-state Interhemispheric functional connectivity. *Journal of Neuroscience*, *30*(11), 3964–3972. https://doi.org/10.1523/JNEUROSCI.5709-09.2010

Verstynen, T., Diedrichsen, J., Albert, N., Aparicio, P., & Ivry, R. B. (2005). Ipsilateral motor cortex activity during unimanual hand movements relates to task complexity. *Journal of Neurophysiology*, *93*(3), 1209–1222. https://doi.org/10.1152/jn.00720.2004

Volz, L. J., Hamada, M., Rothwell, J. C., & Grefkes, C. (2015). What makes the muscle twitch: Motor system connectivity and TMS-induced activity. *Cerebral Cortex*, *25*(9), 2346–2353. https://doi.org/10.1093/cercor/bhu032

Volz, L. J., Rehme, A. K., Michely, J., Nettekoven, C., Eickhoff, S. B., Fink, G. R., & Grefkes, C. (2016). Shaping early reorganization of neural networks promotes motor function after stroke. *Cerebral Cortex*, *26*(6), 2882–2894. https://doi.org/10.1093/cercor/bhw034

Volz, L. J., Sarfeld, A.-S., Diekhoff, S., Rehme, A. K., Pool, E.-M., Eickhoff, S. B., … Grefkes, C. (2015). Motor cortex excitability and connectivity in chronic stroke: A multimodal model of functional reorganization. *Brain Structure and Function*, *220*(2), 1093–1107. https://doi.org/10.1007/s00429-013-0702-8

Volz, L. J., Vollmer, M., Michely, J., Fink, G. R., Rothwell, J. C., & Grefkes, C. (2017). Time-dependent functional role of the contralesional motor cortex after stroke. *NeuroImage: Clinical*, *16*(June), 165–174. https://doi.org/10.1016/j.nicl.2017.07.024

Ward, N. S., Brown, M. M., Thompson, A. J., & Frackowiak, R. S. J. (2003). Neural correlates of motor recovery after stroke: A longitudinal fMRI study. *Brain*, *126*(11), 2476–2496. https://doi.org/10.1093/brain/awg245

Yousry, T. (1997). Localization of the motor hand area to a knob on the precentral gyrus. A new landmark. *Brain*, *120*(1), 141–157. https://doi.org/10.1093/brain/120.1.141

Zheng, X., Sun, L., Yin, D., Jia, J., Zhao, Z., Jiang, Y., … Fan, M. (2016). The plasticity of intrinsic functional connectivity patterns associated with rehabilitation intervention in chronic stroke patients. *Neuroradiology*, *58*(4), 417–427. https://doi.org/10.1007/s00234-016-1647-4

SUPPORTING INFORMATION

Additional supporting information may be found online in the Supporting Information section at the end of this article.

How to cite this article: Paul, T., Hensel, L., Rehme, A. K., Tscherpel, C., Eickhoff, S. B., Fink, G. R., Grefkes, C., & Volz, L. J. (2021). Early motor network connectivity after stroke: An interplay of general reorganization and state-specific compensation. *Human Brain Mapping*, *42*(16), 5230–5243. https://doi.org/10.1002/hbm.25612